

Compressive behaviour of steel fibre reinforced concrete

R. D. Neves and J. C. O. Fernandes de Almeida

An experimental study to investigate the influence of matrix strength, fibre content and diameter on the compressive behaviour of steel fibre reinforced concrete is presented. Two types of matrix and fibres were tested. Concrete compressive strengths of 35 and 60 MPa, 0.38 and 0.55 mm fibre diameter, and 30 mm fibre length, were considered. The volume of fibre in the concrete was varied up to 1.5%. Test results indicated that the addition of fibres to concrete enhances its toughness and strain at peak stress, but can slightly reduce the Young's modulus. Simple expressions are proposed to estimate the Young's modulus and the strain at peak stress, from the compressive strength results, knowing fibre volume, length and diameter. An analytical model to predict the stress-strain relationship for steel fibre concrete in compression is also proposed. The model results are compared with experimental stress-strain curves.



Rui D. Neves

Concrete Division,
Laboratório Nacional de
Engenharia Civil (LNEC),
Lisbon, Portugal



João C. O. Fernandes de Almeida

Civil Engineering
Department, Instituto
Superior Tecnico, Lisbon,
Portugal

Notation

A, B, C	parameters to be determined by regression analysis
d_f	fibre diameter
E_i	Young's modulus
f_c	compressive strength
I_5	toughness index
l_f	fibre length
p, q	parameters related to material's stiffness and ductility
V_f	fibre volume
ϵ	strain
ϵ_0	strain at peak stress
σ	stress

Introduction

The development of concrete technology has made it possible to reach, for ordinary production processes, compressive strengths as high as 100 MPa. However, such an increase in compressive strength is in general associated with brittle behaviour of the concrete. In structural applications brittleness can be prevented

by means of confinement with transverse reinforcement. For structures where ductility is very important, such as seismic-resistant reinforced concrete structures, the design and detailing of confinement reinforcement is often difficult, requiring more labour and quality control and affecting construction costs. The recognised ability of fibres to improve ductility of concrete¹⁻⁵ may be used to overcome that difficulty. Other potential uses of steel fibre reinforced concrete are the compressive layers of block-and-beam and pre-cast permanent formwork floors, or discontinuity regions, where loading paths are complex, such as corbels, deep beams and post-tensioning anchorage zones.

In this context, it is important for designers to know the compressive behaviour of steel fibre reinforced concrete. The aim of the present work was to develop analytical expressions to estimate the main parameters that characterise the behaviour of steel fibre reinforced concrete in compression.

Experimental programme

To evaluate the influence of steel fibres on the compressive behaviour of concrete, two

different mixes and two different fibres were used. Concrete mix proportions are indicated in Table 1. The aggregates were siliceous natural sand and crushed limestone (gradings shown on Figure 1). The steel fibres were hook-ended of length $l_f = 30$ mm, diameter $d_f = 0.55$ mm and $d_f = 0.38$ mm (Table 2), and they were added to the two mixes in volume contents up to $V_f = 1.5\%$.

The concrete was mixed using a laboratory pan-mixer, with mixing times ranging from 3 to 6 min, and compacted on a vibrating table. The compacting time varied between 40 and 60 s, depending on the concrete workability.

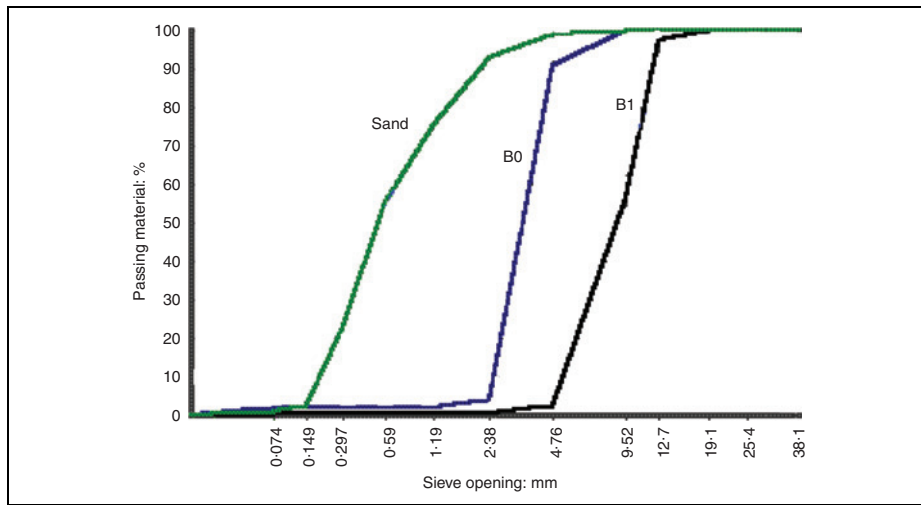
Demoulding occurred 24 h after mixing and then the specimens were kept in a wet chamber until required for testing at 42 days.

As matrix and fibre type and content varied, different composites were tested. Their identification is shown in Table 3, which shows the mix designation (A, B), followed by the fibre content (in kg/m³) and then the fibre type (Z, R). Each composite was represented by a set of six cylinders, 150 mm in diameter and 300 mm in height.

Tests were performed in a closed-loop, servo-controlled compression testing machine with a load capacity of 5000 kN and an

Table 1 Mix design, quantity per m³

Mix	Cement I 42.5R: kg	Fly ash: kg	Plasticiser: litres	Super plasticiser: litres	Water: litres	Sand: kg	Coarse agg. B0: kg	Coarse agg. B1: kg
A	250	70	2.19	–	168	876	250	706
B	450	–	–	5.71	174	682	292	744



△ Figure 1 Aggregate grading

Table 2 Fibre properties

Fibre	Z	R
Ultimate stress: MPa	>1150	>2300
Length: mm	30	30
Diameter: mm	0.55	0.38
Aspect ratio: l_f/d_f	55	80

approximate stiffness of 2300 kN/mm.⁶ Before testing, the two ends of each specimen were made parallel by grinding. The tests were performed under displacement control with a plate displacement rate of 0.01 mm/s, which corresponds to the lowest limit of the interval identified in Ref. 7. To measure the deformations of the specimens and the force, a clamp type extensometer (HBM DD1) and a load cell HBM P3MB were used. The methods used to determine $\sigma-\varepsilon$ curves from load-displacement data and to calculate the average curve

representing each composite are described in Neves.⁸

Test results and analysis

The main parameters that characterise the compressive behaviour of concrete are the slope of the ascending branch (Young's modulus), the compressive strength, the strain at peak stress and the area under the $\sigma-\varepsilon$ curve (toughness). These parameters were determined from the respective average curve

Table 3 Composites identification

Mix design	Fibre type	V_f : %				
		0	0.38	0.75	1.13	1.50
A	Z	A0	A.30.Z	A.60.Z	A.90.Z	A.120.Z
	R		A.30.R	A.60.R	A.90.R	-
B	Z	B0	B.30.Z	B.60.Z	B.90.Z	-
	R		B.30.R	B.60.R	B.90.R	B.120.R

for each composite and are presented in Table 4.

Young's modulus

The test results (Figure 2) illustrate the well-known relation between compressive strength and Young's modulus, and also show that the presence of fibres causes a slight decrease in Young's modulus. Similar behaviour has been reported by other authors^{9,10} and can be explained because fibres parallel to the load direction can act like voids and also due to the eventual additional voids caused by fibre addition.

Considering this variation and the relation of Young's modulus with compressive strength, Mansur *et al.*¹⁰ have proposed an analytical expression of the form

$$E_i = (A - BV_f)f_c^{1/3} \tag{1}$$

Regression analyses for the groups of specimens tested led to the following expression to estimate Young's modulus

$$E_i = (10.5 - 0.22V_f)f_c^{1/3} \tag{2}$$

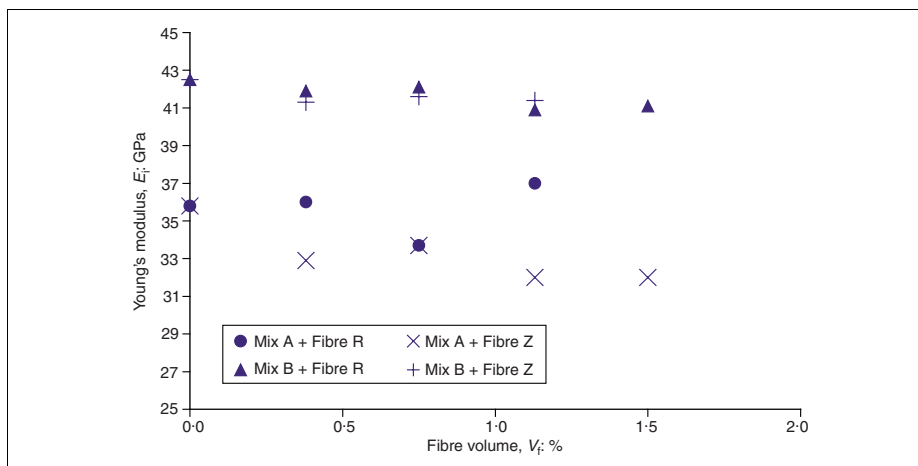
where E_i is expressed in GPa, f_c in MPa and V_f as a percentage. As the origin of the coarse aggregate influences the relation between Young's modulus and compressive strength, for aggregates other than limestone, the presented equation (2) needed to be adjusted.

Compressive strength

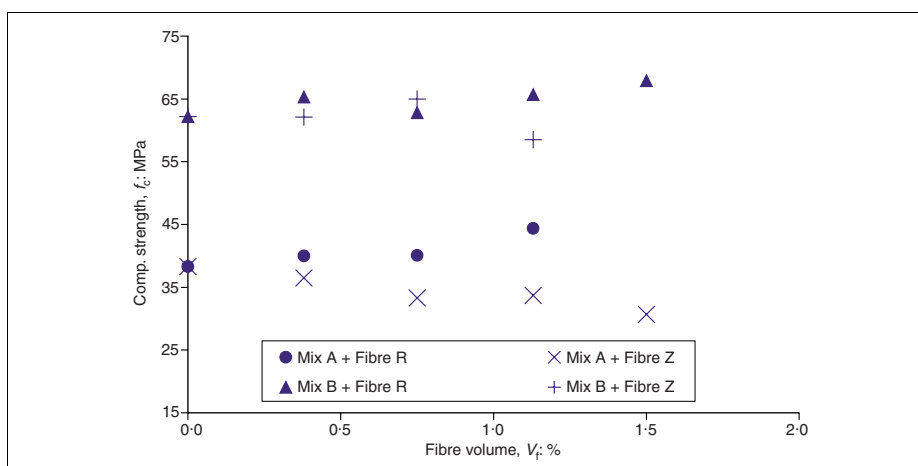
The reinforcement provided by fibres can work at both a micro and macro level. At a micro level fibres arrest the development of microcracks, leading to higher compressive strengths, whereas at a macro level fibres control crack opening, increasing the energy absorption capacity of the composite. Although the primary purpose of fibre reinforcement is to improve energy absorption capacity after macrocracking of the matrix has occurred, this reinforcement often works also at a micro level. The ability of the fibre to control microcracking growth depends mainly on the number of fibres, deformability and bond to the matrix.¹¹ A higher number of fibres in the matrix leads to a higher probability of a microcrack being intercepted by a fibre. If the fibre is

Table 4 Summary of results

Composite	Young's modulus, E_i : GPa	Compressive strength, f_c : MPa	Strain at peak stress: $\epsilon_o (\times 10^{-3})$	Toughness index, I_5
A0	35.8	38.3	1.94	2.61
B0	42.5	62.2	2.38	1.9
A.30.Z	32.9	36.5	1.95	3.22
A.30.R	36.0	40.0	2.07	3.21
B.30.Z	41.3	62.1	2.35	2.65
B.30.R	41.9	65.3	2.42	2.84
A.60.Z	33.7	33.3	2.01	3.42
A.60.R	33.7	40.1	2.29	3.64
B.60.Z	41.6	65.0	2.46	2.93
B.60.R	42.1	62.8	2.53	3.58
A.90.Z	32.0	33.7	2.14	3.57
A.90.R	37.0	44.4	2.33	3.80
B.90.Z	41.4	58.5	2.54	3.43
B.90.R	40.9	65.7	2.95	3.31
A.120.Z	32.0	30.7	2.16	3.58
B.120.R	41.1	67.9	3.01	3.77



△ Figure 2 Young's modulus as a function of fibre content



△ Figure 3 Compressive strength as a function of fibre content

stiff enough and it is well bonded to the matrix, it can prevent the microcrack developing.

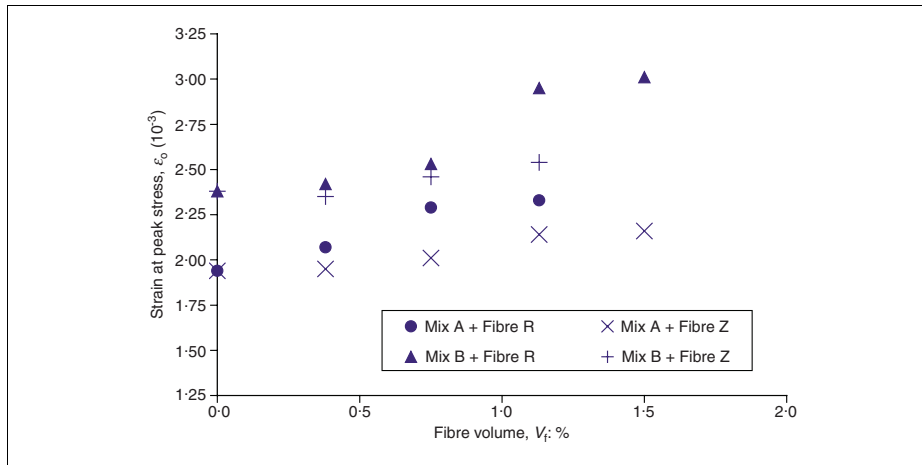
On the other hand, fibre addition causes some perturbation of the matrix, which can result in higher voidage.¹² Voids can be seen as defects where microcracking starts. In addition to fibre quantity, perturbation also depends on the ability of the matrix to accommodate fibres, which is an important property of the mortar fraction of the concrete.

Therefore the influence of fibres on the compressive strength may be seen as the balance between microcrack bridging and additional voids caused by fibre addition. In the present study different influences were observed (Figure 3): the R fibres increased the strength of the composites by up to 9% whereas the Z fibres reduced it by up to 20%.

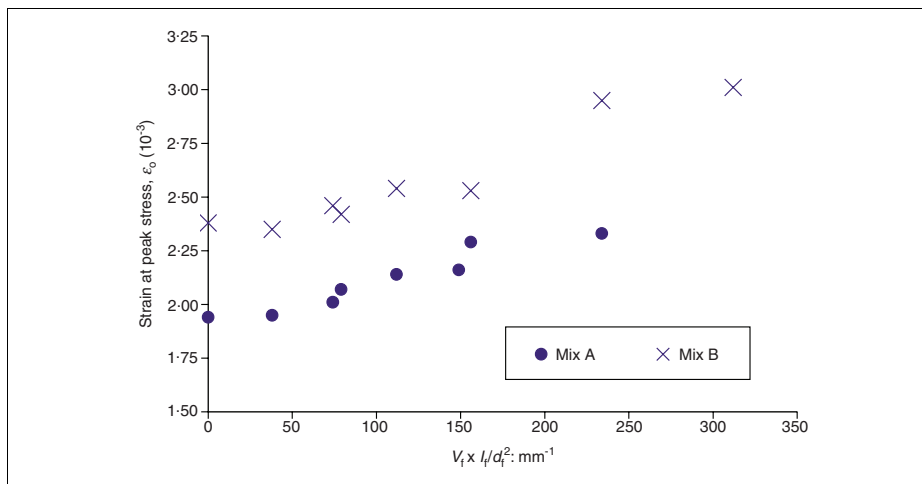
As the compressive strength of the steel fibre reinforced concrete depends not only on the fibre type and volume, but mainly on the mix characteristics and as compression testing is quite simple, it is recommended to evaluate the compressive strength by testing, rather than by analytical expressions.

Strain at peak stress

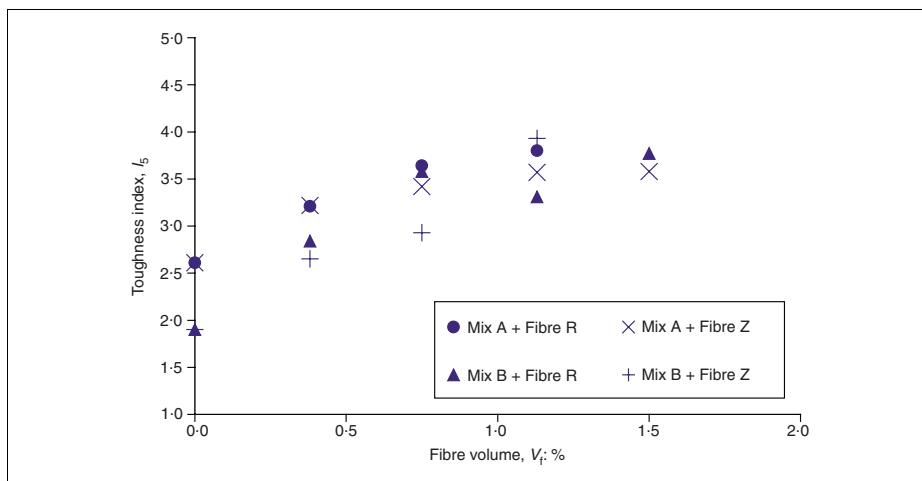
The strains at peak stress obtained in this work (Figure 4) indicate an increase of ϵ_o with compressive strength, as already observed by other



△ Figure 4 Strain at peak stress as a function of fibre content



△ Figure 5 Strain at peak stress as a function of $V_f \times l_f/d_f^2$



△ Figure 6 Toughness index as a function of fibre content

authors.^{10,13,14} Figure 4 also shows a consistent increase of ϵ_0 with fibre volume and a different influence from R and Z fibres.

According to some researchers^{10,15} the fibre influence on strain at peak stress is a function of the reinforcing index [$V_f \times (l_f/d_f)$]. However, a better relation was found using the adherence index,⁸ [$V_f \times (l_f/d_f^2)$] (Figure 5).

In order to find an analytical expression to estimate the strain at peak stress, for given compressive strength and adherence index, the formula proposed by Amziane and Loukili¹⁵ was modified to

$$\epsilon_0 = A \times f_c^{[B+C \times V_f(l_f/d_f^2)]} \quad (3)$$

Regression analyses for the groups of specimens tested led to the following expression to estimate the strain at peak stress

$$\epsilon_0 = 0.69 \times f_c^{[0.29+0.0002 \times V_f(l_f/d_f^2)]} \quad (4)$$

where ϵ_0 is expressed in parts per thousand, f_c in MPa, V_f as a percentage, l_f and d_f in mm.

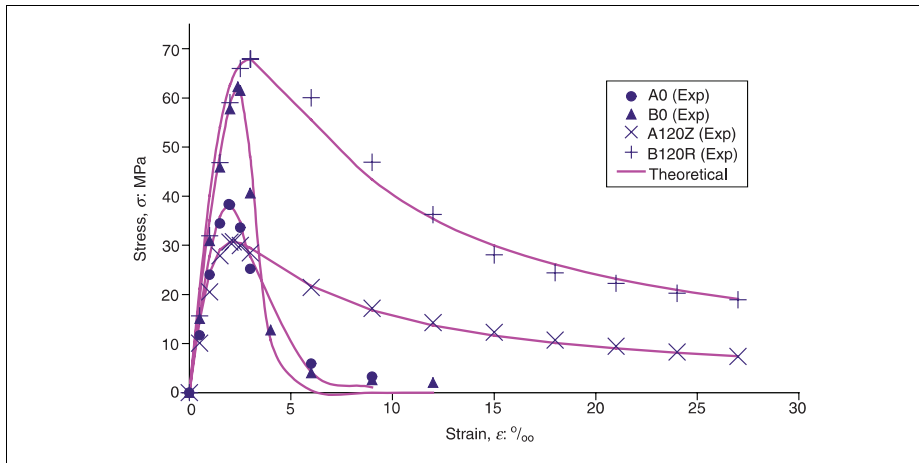
As fibres with different shapes have distinct effects on increasing the strain at peak stress,¹⁶ care should be taken when using equation (4) to estimate ϵ_0 when using fibres other than hook-ended.

Toughness index

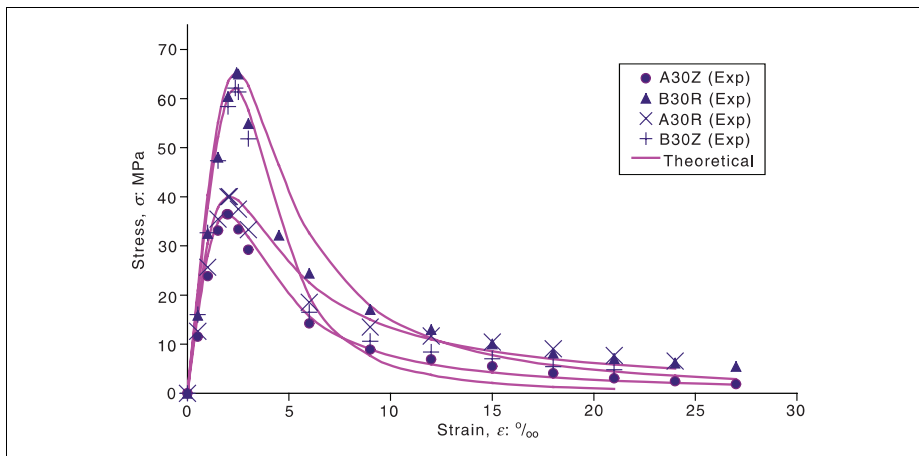
A suitable parameter to quantify the compressive behaviour after peak stress is the toughness index. This parameter can be used as well to define the parabola–rectangle diagram to be used in ultimate limit state (ULS) design.¹⁷ Although this index was originally defined to characterise the flexure energy absorption capacity, it has also been used, with slight modifications, by some authors^{10,18,19} for compressive behaviour. The values presented in Figure 6 were obtained from the average stress–strain curve of each composite by the following formula:

$$I_5 = \frac{\int_0^{\epsilon_0} \sigma(\epsilon) d\epsilon}{\int_0^{\epsilon_0} \sigma(\epsilon) d\epsilon} \quad (5)$$

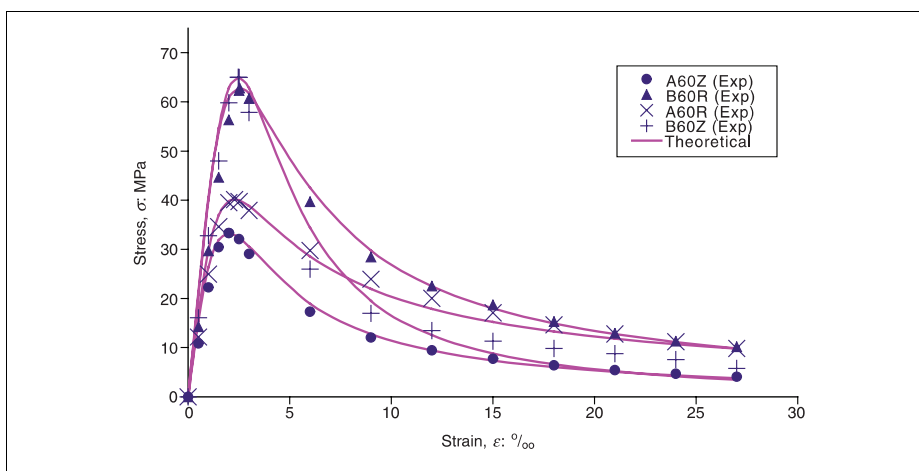
For plain concrete, the toughness index decreases with increasing compressive strength of the concrete, as concrete becomes more brittle as its compressive strength increases. Fibre addition, even in dosages as low as



△ Figure 7 Experimental and theoretical stress–strain curves for plain and $V_f = 1.5\%$ concrete



△ Figure 8 Experimental and theoretical stress–strain curves for plain and $V_f = 0.38\%$ concrete



△ Figure 9 Experimental and theoretical stress–strain curves for plain and $V_f = 0.76\%$ concrete

30 kg/m³, reduced the toughness of the high-strength concrete to values similar to those of ordinary concrete without fibres.

Stress–strain model

There are several models to predict concrete compressive behaviour.^{20–22} These models are in general not suitable for steel fibre reinforced concrete, because steel fibre reinforced concrete composites have a less steep descending branch than plain concrete. Some authors^{10,19} have suggested the adaptation of the Carreira–Chu model²¹ to this type of composite. The best agreement with the present experimental results was obtained when using the model proposed by Vipulanandam and Paul,²³ originally intended to predict the polymer concrete behaviour, based in the following expression

$$\sigma = \frac{\frac{\varepsilon}{\varepsilon_0}}{(1 - p - q) + q\left(\frac{\varepsilon}{\varepsilon_0}\right) + p\left(\frac{\varepsilon}{\varepsilon_0}\right)^{1-q/p}} \cdot f_c \quad (6)$$

in which p and q are material deformability-related parameters to be determined, and should satisfy the following conditions:

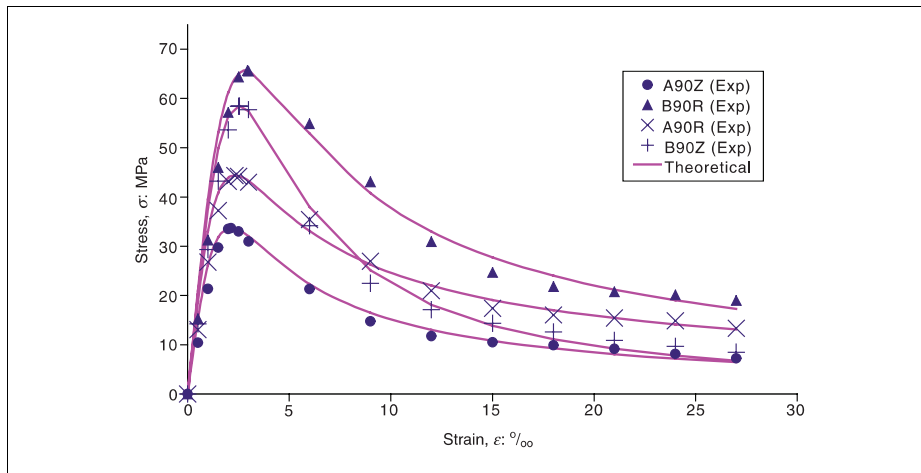
$$p + q = 1 - \frac{f_c}{E_i \varepsilon_0} \quad (7)$$

$$p + q \in]0, 1[\quad (8)$$

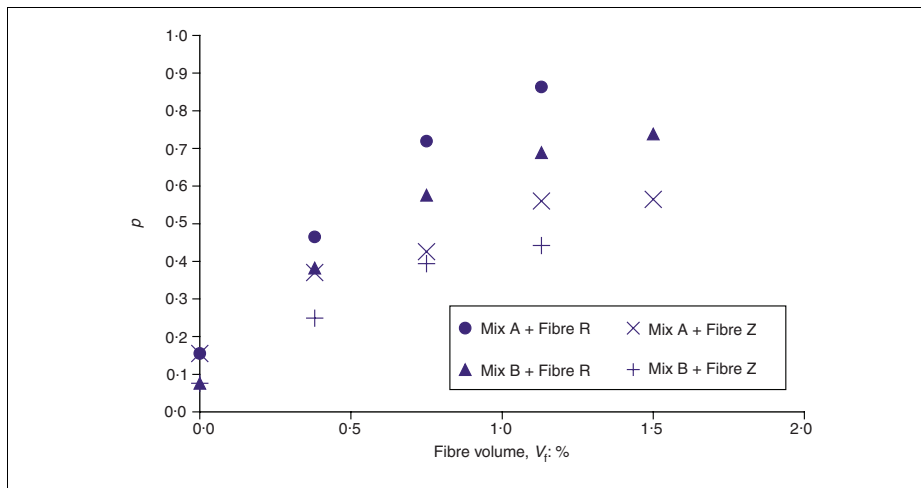
$$\frac{1 - q}{p} > 0 \quad (9)$$

Knowing Young’s modulus, compressive strength and strain at peak stress, one can express q as a function of p , using equation (7), thus reducing to 1 the number of parameters to be determined. Assuming different values for p , and calculating the sum of square errors (SSE) between points of the experimental curve and the points of the analytical one, led to a value of p that minimises the error between both curves. Figures 7 to 10 show the suitability of the proposed expression to model the compressive behaviour of plain and steel fibre reinforced concrete with strengths and fibre volumes up to 60 MPa and 1.5%, respectively.

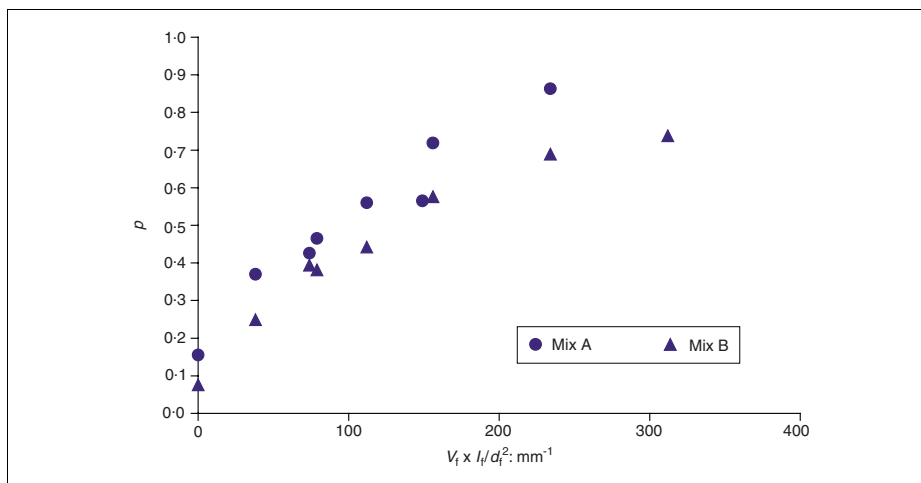
The sets of p values that minimise the error between experimental and theoretical curves of each composite are presented in Figure 11.



△ Figure 10 Experimental and theoretical stress–strain curves for plain and $V_f = 1.13\%$ concrete



△ Figure 11 Values of p as a function of fibre content



△ Figure 12 Variation of p with adherence index

This figure shows the variation of p with fibre volume for different mixes and fibre types.

As occurred for the variation of strain at peak stress, the adherence index [$V_f \times (l_f/d_f^2)$] showed a good correlation with the variation of p (Figure 12).

The variation presented in Figure 12 can be modelled by an analytical expression similar to the one used by Neves⁸

$$p = 1 - A \times f_c^{[B \times V_f (l_f/d_f^2)]} \quad (10)$$

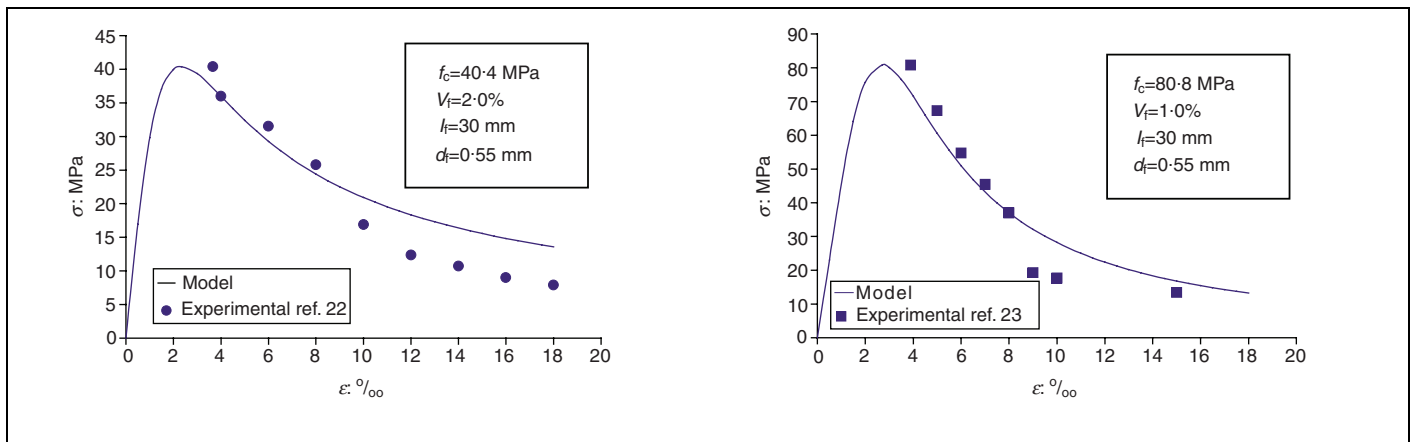
Regression analyses for the two sets of p values indicated that $A = 0.85$ and $B = -0.0013$ and so equation (10) becomes

$$p = 1 - 0.85 \times f_c^{[-0.0013 \times V_f (l_f/d_f^2)]} \quad (11)$$

where p is the parameter to use in the stress–strain model, f_c is the composite compressive strength obtained by testing, in MPa, V_f the fibre volume as a percentage, l_f and d_f the fibre length and diameter in mm. Knowing the compressive strength, the fibre volume and fibre geometrical properties, it is possible to estimate p using equation (11), ε_0 using equation (4), E_1 using equation (2) and then q using equation (7). Introducing these parameters in equation (6) will define an analytical expression to model each composite compressive behaviour.

The ability of the proposed set of expressions to predict the stress–strain curve of steel fibre reinforced concrete, even for concrete with compressive strength up to 80 MPa or fibre volumes up to 2.0% is illustrated in Figure 13. The results presented by Otter and Naaman,²⁴ and Hsu and Hsu,²⁵ are compared with the theoretical behaviour given by the proposed model.

It should be pointed out that the results presented in Refs 24 and 25 were also obtained for concrete reinforced with hook-end steel fibres. However, when comparing the proposed model application with the results from other researchers using different experimental conditions, namely straight fibres or smaller specimens, such as cylinders with 100 mm diameter and 200 mm height, the agreement was not so good. So, in situations in which the fibres are of different shape, different specimens or even different coarse aggregate is used, the proposed model needs further calibration.



△ Figure 13 Model prediction for concretes tested by other authors

Concluding remarks

The influence of matrix strength, fibre content and diameter on the steel fibre reinforced concrete compressive behaviour was studied. Within the range of the considered variables in this investigation, the authors may point out the following conclusions.

- Young's modulus shows a slight tendency to decrease as fibre content increases.
- Fibre influence in maximum compressive strength it is variable, depending on matrix and fibre characteristics.
- Strain at peak stress increases with concrete strength.
- The increase of strain at peak stress also showed a good agreement with the increase of $[V_f \times (l_f/d_f^2)]$, designated as adherence index.
- Toughness of higher strength concrete is more sensitive to fibre reinforcement.
- The stress-strain relationship presented by Vipulanandam and Paul is suitable to model the compressive behaviour of the tested steel fibre reinforced concretes.
- Equations (2), (4) and (11), proposed in this work, together with equations (7) and (6), enable modelling the steel fibre reinforced concrete behaviour in uniaxial compression.
- However, the validity of the proposed model should be checked when using different experimental conditions, mainly the post peak branch for fibres other than hook-ended.

References

- American Concrete Institution. *State-of-the-Art Report on Fiber Reinforced Concrete*. ACI Manual of Concrete Practice, Part 5. ACI International, Farmington Hills, 1998.
- Swamy, R. Structural implications of high performance fibre cement composites. In *High Performance Fiber Reinforced Cement Composites* (eds H. Reinhardt and A. Naaman). E&FN Spon, London, 1992.
- Naaman, A., Wight, J. and Abdou, H. SIFCON connections for seismic resistant frames. *Concrete International*, 1987, **9**, No. 11, 34–39.
- Rossi, P. Steel fiber reinforced concretes (SFRC): an example of French research. *Materials Journal*, 1994, **91**, No. 3, 273–279.
- Shah, S., Peled, A. and Aldea, C. Scope of high performance fiber reinforced cement composites. In: *High Performance Fiber Reinforced Cement Composites* (eds H. Reinhardt and A. Naaman). RILEM, Bagneux, 1999.
- Neves, R. *Measuring Deformations on Concrete Compression Tests*. Report 13/00-NAB. LNEC, Lisbon, 2000 (in Portuguese).
- The Japan Society of Civil Engineers. Part III-2 Method of Tests for Steel Fiber Reinforced Concrete. *Concrete Library of JSCE*, No. 3. JSCE, Tokyo, 1984.
- Neves, R. *Modeling the compressive behaviour of steel fibre reinforced concrete*. MSc Thesis. IST, Lisbon, 2000 (in Portuguese).
- Rossi, P. and Harrouche, N. Mix design and mechanical behaviour of some steel fibre-reinforced concretes used in reinforced concrete structures. *Materials and Structures*, 1990, **23**, No. 136, 256–266.
- Mansur, M., Chin, M. and Wee, T. Stress-strain relationship of high-strength fiber concrete in compression. *Journal of Materials in Civil Engineering*, 1999, **11**, No. 1, 21–29.
- Rossi, P. *Les Bétons de Fibres Métalliques*. Presses ENPC, 1998.
- Neves, R. and Gonçalves, A. *Steel Fibre Reinforced Concrete—Durability Related Properties*. LNEC, Lisbon, 2000 (in Portuguese).
- Nicolo, B., De, Pani, L. and Pozzo, E. Strain of concrete at peak compressive stress for a wide range of compressive strengths. *Materials and Structures*, 1994, **27**, No. 168, 206–210.
- Taerwe, L. Influence of steel fibres on strain-softening of high-strength concrete. *Materials Journal*, 1992, **88**, No. 6, 54–60.
- Amziane, S. and Loukili, A. Étude expérimentale du comportement des bétons à hautes performances renforcés de fibres d'acier sous chargements statique et cyclique. *Materials and Structures*, 1999, **32**, No. 219, 348–353.
- Soroushian, P. and Bayasi, Z. Fiber-type effects on the performance of steel fiber reinforced concrete. *Materials Journal*, 1991, **88**, No. 2, 129–134.
- Taerwe, L. and Van Gysel, A. Influence of steel fibres on design stress-strain curve for high-strength concrete. *Journal of Engineering Mechanics*, 1996, **122**, No. 8, 695–704.
- Mebarkia, S. and Vipulanandan, C. Compressive behavior of glass-fiber-reinforced polymer concrete. *Journal of Materials in Civil Engineering*, 1992, **4**, No. 1, 91–105.
- Hsu, L. and Hsu, C.-T. Stress-strain behaviour of steel-fiber high strength concrete under compression. *Structural Journal*, 1994, **91**, No. 4, 448–457.
- Comité Européen du Béton/Fédération Internationale de la Précontrainte. *Model code 1990*. Thomas Telford, London, 1993.

21. Carreira, D. and Chu, K. Stress-strain relationship for plain concrete in compression. *ACI Journal*, 1985, **83**, No. 6, 797–804.
22. Yip, W. Generic form of stress-strain equations for concrete. *Cement and Concrete Research*, 1998, **28**, No. 4, 499–508.
23. Vipulanandan, C. and Paul, E. Performance of epoxy and polyester polymer concrete. *Materials Journal*, 1990, **87**, No. 3, 241–251.
24. Otter, D. and Naaman, A. Properties of steel fiber reinforced concrete under cyclic loading. *Materials Journal*, 1988, **85**, No. 4, 254–261.
25. Hsu, L. and Hsu, C.-T. Stress-strain behaviour of steel-fiber high strength concrete under compression. *Structural Journal*, 1994, **91**, No. 4, 448–457.